Slimi, B.; Ben Assaker, I.; Kriaa, A.; Marí, B.; Chtourou, R. (2017). One step electrodeposition of Ag-decorated ZnO nanowires. Journal of Solid State Electrochemistry. 21(5):1253-1261. doi:10.1007/s10008-016-3476-0.

One step electrodeposition of Ag-decorated ZnO nanowires

B. Slimi[a,b,*], I. Ben Assaker[a], A. Kriaa[c], R. Chtourou[a], B. Marí[d]

[a] Laboratoire Photovoltaïques, Centre de Recherches et des Technologies de l'Energie Technopole Borj Cedria, Bp 95, Hammam Lif 2050, Tunisie
[b] Faculté des Sciences de Bizerte, Université de Carthage, Tunisie
[c] Laboratoire de Chimie Moléculaire Organique, 5 Avenue Taha Houssein Monfleury, 1089 Tunis, Tunisie
[d]Departament de Física Aplicada. Universitat Politècnica de València, Camí de Vera s/n 46071 València, Spain

* Corresponding author: bechir.slimi0511@gmail.com

Abstract:

Pure and Ag-decorated ZnO nanowires (ZnO NWs) were grown by electrodeposition technique onto ITO conductive glass substrate. A new contribution to the knowledge of Ag dependence of morphological, structural, optical properties is reported, as well as the electrochemical behavior of the ITO/Ag-ZnO NWs electrode/Na_2SO_4 electrolyte solution interface. X-ray diffraction revealed that the all samples are mainly crystallized in wurtzite ZnO phase. The scanning electron microscopy images show that in the absence or presence of Ag, nanowires appear uniform and stand perpendicular onto substrate with hexagonal shape implying the occurrence of the wurtzite ZnO crystal structure. The presence of Ag nanoparticles is clearly envisioned by EDX spectra. The obtained results According to optical measurements the band gap for undoped ZnO NWs is about 3.25 eV, close to that of ZnO (films, powder and nanorods) 3.36 eV. Optical absorption shows a surface Plasmon resonance effect at 400 nm and 550 nm. Microanalysis confirmed that the amount of Ag in thin solid films is proportional to the Ag content in the starting electrolyte. The increase of Ag-doping results in a decrease of the photoluminescence intensity and blue shift and has been assigned to the Plasmon effect of Ag. Photoelectrochemical measurements showed that the photocurrent increases from 0.05 mA for undoped ZnO NWs to 0.14 mA for the 3% Ag-decorated ZnO NWs.

Keywords: Ag decorated ZnO Nanowires; Electrodeposition technique; Photoelectrochemical application.

Introduction

ZnO is a semiconductor material belonging to the II-VI family with direct band gap energy (3.37 eV) and a large exciton binding energy (60 meV) at room temperature [1-7]. Recently, one-dimensional (1D) ZnO nanostructures such as nanowires, nanorods (short nanowires), nanofibres, nanobelts and nanotubes have been of an intense interest in both academic research and industrial applications because of their potential as building blocks for other structures [8-10]. Due to their remarkable performance in electronics, optics and photonics, ZnO nanowires are considered as an attractive candidates for many applications such as UV lasers [11], light-emitting diodes [12], photocatalysts [13], nanogenerators [14], gas sensors [15], photodetectors [16]. Recently, an immense attention has focused on the preparation of ZnO nanowires and their applications as photoanode in solar cell [17]. Since UV light accounts for only 3-5% of the sunlight, the wide band gap character of pure ZnO photoanode limits the utilization of complete solar energy. Visible-light driven photoanode cell have attracted much attention recently [18]. For this reason, doping is an effective way to improve the properties of ZnO nanowires. Therefore, adding suitable doping elements to ZnO paves the way for enhancing and controlling its optical and electrical properties, which is crucial for practical applications. Several elements have been added to ZnO for improving its PEC performance [17]. Recent studies have shown that some semiconductors can be used as active material to be loaded with noble metals such as Ag–ZnO [19], Au–ZnO [20], Pt-ZnO [21] and Al-ZnO [22], providing an exciting area for the functionality of materials and new designs of structures carrying electrical signals. It exhibits shift in the Fermi level to more negative potential, resulting in the enhancement of the efficiency of interfacial charge-transfer process. Such metal-semiconductor composite can play an important role in improving the performance of photoelectrochemical (PEC) solar cells, with effect of Surface Plasmon Resonance (SPR). More recently, silver especially has attracted intense interest because of its efficient SPR in the visible light region. Moreover, the metallic Ag could effectively facilitate efficient charge separation, and thus suppress the recombination of photoexcited electron-hole pairs and improve the photoelectrochemical performances.

In fact, several methods have been used to synthesize Ag doped ZnO nanowires such as, chemical vapor deposition (CVD) [23], physical vapor deposition (PVD) [24], hydrothermal method [25], thermal evaporation [26] and electrodeposition [27, 28], and so on. Among these methods, the electrochemical deposition method has attracted the most interest due to its ability to produce integrative, vertically oriented nanowires arrays with controllable dimensions [29] and does not require complex procedures, advanced equipment and delicate

experimental conditions [30]. T. Pauporté and al [31] have prepared Ag-doped ZnO nanowire arrays at low temperature by electrodeposition technique and have studied the application to light emitting diode. O. Lupan and al [32] have synthesized arrays of crystalline ZnO:Ag nanowires by electrodeposition technique onto F-doped tin oxide coated substrates. They found that ZnO:Ag nanowires based nanosensor possesses a much faster response/recovery time and a higher response to UV radiation and hydrogen gas.

To best of our knowledge, there are few report in the literature that have studied the silver doping effect on the electrochemical behavior of electrodeposited Ag-decorated ZnO nanowires. For this reason, in the present work, nanostructure Ag-decorated ZnO onto indium tin oxide (ITO) coated substrate was synthesized by only one step electrodeposition method. The research was focused on the influence of percentage of silver on the structural, morphological, optical and electrical properties. The aim of the study was to show how the silver affects the characteristics of PEC measurements.

2. Experimental

2.1. Electrodeposition of pure and Ag-decorated ZnO nanowires

Electrodeposition of pure ZnO nanowires onto indium tin oxide (ITO) coated glass substrate from aqueous solution has been reported earlier by our group [29, 33, 34]. The synthesis was carried out using an Autolab PGSTAT30 potentiostat/galvanostat in a standard three-electrode system. The working electrode was an ITO coated glass substrate while the counter electrode and the reference one were a Pt wire and an Ag/AgCl electrode, respectively. The Electrolyte bath was composed by an aqueous solution of $ZnCl_2$ (5.10^{-4} M) and KCl (0.1 M) as a supporting electrolyte and a continuous bubbling of oxygen was kept during the electrodeposition process. The temperature was adjusted to 80 °C with an applied potential of -1.0 V vs. Ag/AgCl for 7200 s.

To obtain the Ag-decorated ZnO nanowires, silver nitrate ($AgNO_3$) was used as doping source and added to the electrolyte bath. The Ag decorated ratio defined by [Ag]/[Zn] varied over a range of 0-3%. The electrodeposition of Ag-decorated ZnO NWs was performed onto ITO substrate using same conditions.

2.2. Characterizations of pure and Ag-decorated ZnO NWs

The as-prepared ZnO NWs and Ag-decorated ZnO NWs were examined by various characterization techniques. The morphology and the chemical composition of the samples were studied using a Philips CM20 (FESEM-7500 F.ULTRA 55) instrument operating at 200 kV equipped with Energy Dispersive X-ray Spectrometer (EDX) mounted on a scanning

electron microscope (SEM). The crystalline structure of the as-prepared samples was determined by X-ray diffraction (XRD) using a Bruker D8 advance diffractometer with Cu K_α (λ = 1.541 Å) X-rays at 45 kV and 40 mA in the range of 2θ=15–70° with scan speed of 8º/min. The optical properties of the samples were examined by UV-Vis spectroscopy and photoluminescence (PL). The UV−Vis absorption spectrum was recorded in the range of 200-900 nm using the Lambda 900 Perkin Elmer spectrophotometer. Photoluminescence (PL) measurements were recorded at room temperature. It was performed by exciting with the frequency of a pulsed laser (5145 Å) at a typical power density of ≈7 W cm^{-2} and detected through a 266 nm Jobin-Yvon monochromator.

The photoelectrochemical (PEC) measurements of pure ZnO NWs and Ag-decorated ZnO NWs were done using Pt wire and Ag/AgCl as counter and reference electrode, respectively, emerged in a solution of Na_2SO_4 (0,5 M) under light intensity of 200 mW/cm^2 (300 W Xe lamp) . Linear sweep voltammograms were measured under a bias voltage between -1 V and +0.8 V (vs. SCE) with a scan rate of 0.01 V s^{-1}. Amperometric *I–t* curves were tested at a bias voltage of +0.5 V (vs. SCE).

3. Results and discussions

3.1. Morphology

In order to study the effect of Ag on the morphological of ZnO nanowires, the surface morphology of samples was analyzed using scanning electron microscopy (SEM). The SEM micrographs depicted in Figure 1 illustrate the similar morphology of undoped and Ag-decorated ZnO nanowires. The film consists of a dense array of hexagonal ZnO nanowires. The wires are uniformly and compactly aligned approximately normal to the ITO substrate. As for any SEM image obtained with different percentage of silver that be clearly nanoparticule the Ag paste on ZnO nanowires. The diameter and length of undoped and Ag-decorated ZnO nanowires vary from 100-300 nm for the diameter and length of 1200 nm. The diameter and the length of the ZnO nanowires did not change with Ag-coating, but the prepared nanowires are influenced by the temperature deposition and the nature of the substrate to the consumption rate of growth ZnO. The growth rate of nanowires sidewalls and nanowires density [35, 36]. Tips of the nanowires are observed to have a predominantly hexagonal structure, in good agreement with results obtained by Wang et al. [37]. The elemental composition of as-prepared nanowires was examined by EDX and XRD.

EDX analysis of pure ZnO and Ag-decorated ZnO NWs is represented in Fig. 2. EDX confirms the presence of the elements Ag, Zn and O. The results demonstrate that the amount

of Ag has great effect on the morphology of ZnO:Ag NWs. On the condition of small amount of Ag precursors, Ag may be disperse on the surface of ZnO NWs, but ZnO NWs has bended and formed the bundle with increasing the amount of Ag with at 3%. The signals of both Zn and O are attributed to the ZnO NWs. The Ag signal results from the Ag nanoparticles on the surface of the ZnO NWs. No other signals were observed in the EDX, indicating that the as prepared sample is pure.

3.2. Structural properties

Fig. 3 shows the XRD patterns of undoped and Ag-decorated ZnO nanowires grown onto ITO substrate by electrodeposition method with different Ag percentage. These spectra show well-defined peaks of (100), (002), (102), (110), (103) and (112) planes were fully indexed and attributed to single phase of wurtzite ZnO (JCPDS 036-1451). We note also from all the spectra, a peak observed at 34.40° and attributed to (002) plane was relatively much more intense than the others peaks indicating clearly a preferred c-axis orientation of ZnO nanowires. This result is in good agreement with those published in the literature [29,34,38]. In addition, for samples prepared using 2 and 3% as silver content there are two small peaks corresponding to cubic metallic silver located respectively at 38.5° and 44.6° and assigned to (111) and (200) planes [39], indicating the formation of crystalline silver clusters. This behavior was also observed by some authors in the literature. In fact N.L. [17] have obtained Ag-ZnO thin films by using pneumatic spray pyrolysis technique and have demonstrate that the intensity of the peaks (200) increasing with the percentage of the silver in the solution. This phenomena was also obtained by Chi-Jung Chang [40] ho have synthesized Ag-doped ZnO nanorods on stainless-steel wire meshes by chemical bath deposition technique.

In the other hand from figure 3b, one can be clearly observe that compared with undoped ZnO nanowires a slight shift toward smaller angle is found with the increasing of percentage of silver. This behavior have been explaining by many authors and related to the increase of the lattice constants which are caused by substitution of Zn^{2+} ions (ionic radius 0.74 Å) with larger Ag^{+} ions (ionic radius 1.26 Å) [17, 25, 40].

The grain size (D) of the ZnO nanowires through (002) orientation was determined by Debye-Scherer′s formula Eq. (1) [41]:

$$D = \frac{K\lambda}{\beta \cos\theta} \qquad \text{Eq. (1)}$$

Where $K = 0.89$, D represents the mean size of the crystallite, β is the observed angular width at half maximum intensity (FWHM) of the (002) peak, λ is the X-ray wavelength of CuK_α radiation (1.541 Å) and θ is the Bragg angle. The calculated values of the crystallite size have

been summarized in Table 1 and presented in figure 3c. As shown in this figure that the grain size decreased from 103 nm to 72 nm, with the increasing of Ag content from 0 to 3%. However, FWHM increased with the increasing of Ag content from 0 to 3%. This exhibits a similar tendency as obtained by M.H. Hsu [40]. Finally, the microstrain (ε), which is an interesting structural parameter of Ag-decorated ZnO nanowires synthesized by electrodeposition , is calculated using the following equation Eq. (2) [42]:

$$\varepsilon = \frac{\beta\ 1/2}{4\tan\theta} \qquad \text{Eq. (2)}$$

Where $\beta_{1/2}$ is the full-width half-maximum of (002) peak and θ is the Brag angle. Contrary to grain size, the microstrain increased from 20.49×10^{-4} to 29.13×10^{-4} when the silver concentration increases from 0 to 3% (Table 2 and Fig. 3c). The increased in the strain parameter may be due to a decrease in the grain size, which is influenced by the ionic radius of the Zn^{2+} (0.074 nm) and Ag^{+} (0.126 nm). Ag-doping to decrease the lattice parameters "*a*" "*c*" of the wurtzite structure ZnO. decreased the lattice parameters *a* and *c* to 3.250 and 5.208 Å, respectively, has been determined when Zn^{2+} ions were replaced by Ag^{+} ions because of the larger radius of Ag^{+} ions (0.126 nm) than Zn^{2+} ions (0.074 nm). Decreasing lattice parameters could be caused by either interstitial incorporation of Ag ions into the lattice or Ag ion substitution of the Zn ion.

3.3. Optical studies

The optical properties of undoped and Ag-doped ZnO nanowires were determined from transmission measurements in the range of 200-1500 nm using an UV-Vis-NIR spectrophotometer in order to determine the band gap value of the material. The absorption coefficient (α) of the deposited films is calculated from the observed absorbance and transmittance values using the following Eq. (3) [43]:

$$\alpha = \frac{1}{d}\ln(\frac{A}{T}) \qquad \text{Eq. (3)}$$

Where α is the absorption coefficient in cm^{-1}, d is the film thickness, T is transmittance and A is the absorbance. The nature of transition is determined using the following Eq. (4) [44]:

$$\alpha h\nu = A(\ h\nu - E_g\ )^n \qquad \text{Eq. (4)}$$

where A is an energy dependent constant, E_g is the band gap of the material, $h\nu$ is photon energy, and n is an index that characterizes the optical absorption process and it is theoretically equal to 2, 1/2, 3 or 3/2 for indirect allowed, direct allowed, indirect for-bidden and direct for-bidden transitions. The band gap values were determined from the intercept of

the straight-line portion of the $(\alpha hv)^2$ against the hv graph on the hv-axis at $\alpha = 0$. Fig.4. Shows the transmittance spectra as a function of the wavelength for the undoped and Ag decorated ZnO nanowires deposited onto ITO glass substrate by simple electrodeposition technique. It can be seen from this figure, that undoped ZnO NWs showed a high transmission at wavelength longer than 380 nm. The high transparency in the visible region is a consequence of the wide band gap of the semiconductor (3.27 eV) [31]. After the silver addition the transmittance of Ag-ZnO nanowires in the visible region decreases from 60 to 5% as the Ag doping percentage increases. This observation was also obtained N.T Tarwai et al [17]. They have explained this behavior by the grain boundary scattering and the absorption of the visible light by the Surface Plasmon Resonance (SPR) related to the presence of Ag nanoparticles.

The optical absorption spectra for the samples were also recorded over wavelength range 300-900 nm (Fg.4b). It can be seen clearly that all the spectra have a strong absorption in the UV region, due to the fundamental absorption edge of ZnO corresponding to the band gap energy of wurtzite structure (3.27 eV). After the addition of the silver into Ag-decorated ZnO nanowires, the light absorbance was significantly red-shifted to the visible region. Also, we note from fig.4b the presence of an absorption peak within the range 450-600 nm which is related to the SPR of the silver. This peak is an intense for the sample doped with 3% Ag.
Fig.5. Shows the $(\alpha hv)^2$ vs hv plot of pure ZnO and Ag decorated ZnO nanowires obtained with different Ag concentrations 0, 1, 1.5, 2, and 3 at.% in the solution bath. The band gap measured was found about 3.27 to 3.12 eV. These values are in agreement with that reported in the literature for pure ZnO and Ag–doped ZnO thin films [17, 45]. The decreasing in the band gap with the increasing of Ag contents was related to the substitution of Ag^{+} into Zn^{2+}. This result was in good agreement with the XRD patterns.

However, the optical absorption of ZnO/Ag is not only a simple superposition of SPR and exciton peaks. When there is a direct contact between a semiconductor and a metal, the transfer of electrons occurs among them due to their difference in Fermi energy and it continues until the two systems reach the equilibrium [46]. Another reason for the shift of the plasmon resonance is attributed to the increase in the dielectric constant of the surrounding medium due to the presence of ZnO NWs on top of Ag nanoparticles [47]. However, Xu et al [48] were found that the incorporation of Ag had almost no influence on the optical band gap of ZnO thin films. In conclusion, the optical band gap of ZnO NWs was strongly dependent on the location of Ag nanoparticles with respect to ZnO NWs, which was in turn dependent on film deposition methods.

3.4. Photoluminescence properties

To confirm the optical result, the photoluminescence measurements were performed under exciting with the frequency of a pulsed laser. Fig. 5 shows the photoluminescence (PL) spectra of pure and Ag-decorated ZnO nanowires electrodeposited onto (ITO)-coated glass substrates with different Ag concentrations 0, 1, 1.5, 2 and 3 at %. In all measurement, the excitation wavelength was 266 nm at room temperature. As can be seen from this figure, ZnO nanowires exhibit characteristic emission peak centered at about 3.25 eV witch assigned to the recombination of electron–hole pairs in the semiconductor through an exciton-exciton collision process also the broad peak was caused by surface states or oxygen vacancies [49]. These results are in accordance with the works of H. R. Liu and al [50]. Upon Ag addition in the ZnO nanowires, a red shift in the wavelength and a decrease in the intensity of UV emission peak were observed. This behavior was attributed to the oxygen vacancies in Ag-decorated ZnO NWs and electron transfer from ZnO to Ag on the interface, respectively. The sample Ag-decorated ZnO (3%) showed the minimum PL intensity, caused by the bottom energy level of the conduction band of ZnO was higher than the new equilibrium Fermi energy level (E_f) of Ag/ZnO [51], the photoexcited electrons in the conduction band could transfer from ZnO to Ag nanoparticles, causing the reduction in combination with electrons and holes for ZnO, which results in the decrease of the PL intensity in Ag-decorated ZnO NWs system. With the increase in Ag content, more metal sites were formed and available to accept electrons, which led to a corresponding increase in separation effects for the photoinduced electrons and holes, and reduction in intensity of PL emission. Nonetheless, when the Ag content exceeded the value (as sample Ag-decorated ZnO NWs (1 % Ag)) the PL intensity was decreased. This was attributed to the absorption or reflection of emission at the interface between ZnO and Ag, which was mainly induced by the strong surface plasmon absorption of Ag particles. The interfacial interaction between ZnO and Ag nanoparticles got weakened, which, in a certain degree, improved the possibility of recombination between holes with electrons.

3.5 Photo electrochemical performance

As well known, the photocurrent response is a useful technique to evaluate the separation efficiency of photogenerated electron-hole pairs. The photoresponses of glass/ITO/Ag-ZnONws/Pt cells were carried out by potentiostatic ($I-V$) measurements under xenon lamp

illumination in aqueous solution containing 0.5 M Na_2SO_4 (pH= 7) with applied potential ranging from -0.5 to +0.8 V vs. Ag/AgCl.

As shown in Fig 6 (a and b), for pure ZnO nanowires the observed dark current density was negligible. However, when the Ag content was increased, the spectral response in dark PEC cell gives some dark cathodic current. The origin of this current could generally be correlated with the open circuit voltage and the surface states modifications. Upon illumination of the junction and when the applied voltage (V vs. Ag/AgCl) becoming more positive, the photoenhancement current density of all samples also increased, which is a characteristic of a semiconductor with n-type conductivity. Moreover, we found considerable variation with the addition of Ag content particularly in the short circuit current *Jsc*. As can be seen, a large increase in short-circuit current is accompanied by a slight decrease in open-circuit voltage. The lower value of the Jsc is observed for the pure ZnO nanowires. This may be explained by the easy recombine of the photogenerated electrons and holes. Similar behavior was also reported by others authors such as Tarwal and al. [17].The increment in the current value (*Jsc*) with the increasing of Ag percentage can be explained through the high absorption of Ag-decorated ZnO nanowires related to the Ag nanoparticules and also the energy transfer mechanism from noble metal to ZnO. This greatly reduces the recombination losses of photogenerated charge carriers due to decrement in grain boundary resistance in the charge transportation process [52]. These results are consistent with the Photoluminescence results.

In addition, as shown in Fig. 7, the photoresponses of both pure ZnO NWs and Ag-decorated ZnO NWs electrodes were carried out by potentiostatic (current vs time, *I-t*) measurements using intermittent illumination with total test duration of 300 seconds, under a bias of 0.5 V against an Ag/AgCl reference electrode. Fig.7 demonstrates that the photocurrent of the 3 % Ag-ZnO NWs electrodes is about 0.14 $mA \cdot cm^{-2}$, three times as high as that of pure ZnO NWs (0.045 mA/cm^2). The photocurrent value decreased to zero when the incident light on the photoanode was turned off and returned to its original value only when the light was turned on again. This observation confirms the rapid charge transport after addition of Ag nanoparticules onto ZnO nanowires.

According to the above results, the enhanced PEC properties of Ag decorated ZnO nanowires can be understood by two important reasons. First, the homogeneous deposition of Ag, which reduces the recombination of photogenerated charge carriers. Second, with appropriate absorption spectrum, Ag-ZnO nanowires electrodes can harvest more solar light

and more electron hole pairs could be generated, which would lead to higher photocurrent [25, 32].

As the result shown in this work, it can conclude that the Ag-decorated ZnO NWs obtained by one step electrodeposition process shows remarkable influence on the photocurrent, and gives a considerable improvement in photoelectrochemical performance as compared to pure ZnO nanowires electrode.

6. Conclusions

In this work, vertical Ag-decorated ZnO nanowires with excellent uniformity were successfully synthesized on (ITO)-coated substrate using only one step electrodeposition methods. XRD, SEM and EDX confirm the formation of nanostructure of ZnO with the presence of Ag dopant. From optical measurements, it was found that Ag doping leads to a decrease of the band gap energy and the SPR phenomena was observed.

The PEC performances of the Ag-decorated NWs are improved compared to the pure ZnO NWs. The sample Ag-decorated (3% Ag) shows the highest current as compare to other samples. Also our results suggest the viability of electrodeposition technique for the synthesis of Ag-ZnO NWs. Such electrodeposited Ag-decorated NWs with novel SPR phenomena can be useful for harvesting the visible light in solar cells.

Acknowledgments

B.S. acknowledges the Photovoltaic Laboratory, Center for Research and Technology of Energy Technopole Borj Cedria for financial support. This work was supported by Ministerio de Economía y Competitividad (ENE2013-46624-C4-4-R) and Generalitat valenciana (Prometeus 2014/044).

References

[1] Morrison SR (1967) J Chem Phys 47:1543

[2] Studenikin SA, Golego N, Cocivera M (1998) J Appl Phys 83:2104

[3] Look DC, Reynolds DC, Hemsky JW, Jones RL, Sizelove JR (1999) J Appl Phys Lett 75: 811

[4] Ng HT, Han J, Yamada T, Nguyen P, Chen YP, Meyyappan M (2004) J Nano Lett 4:1247

[5] Janotti A, Van de Walle CG (2009) Rep Prog Phys 72:126501

[6] Chang PC, Fan ZY, Chien CJ, Stichtenoth D, Ronning C, Lu JG (2006) Appl Phys Lett 89:133113

[7] Wang XD, Song JH, Liu J, Wang ZL (2007) Science 316:102-105

[8] Tan ST, AlZayed NS, Lakshminarayana G, Naumar F, Umar AA , Oyama M, Myronchuk G, Kityk IV (2014) Physica 61:23–27

[9] Thomas MA, Sun WW and Cui JB (2012) J Phys Chem C 116:6383 −6391

[10] Yin X, Que W , Fei D, Shen F, Guo Q (2012) J of Alloys and Compounds 524:13–21

[11] Wen LB, Huang YW, Li SB (1987) J Appl Phys 62:2295

[12] Gurav KV, Fulari VJ, Patil UM, Lokhande CD, Joo OS (2010) Appl Surf Sci 256:2580

[13] Kong XY, Wang ZL (2003) Nano Lett 3:1625

[14] Kim K, Song YW, Chang S, Kim I, Kim S, Lee SY (2009) Thin Solid Films 518:1190-1193

[15] Guo Z, Zhao D, Liu Y, Shen D, Zhang J, Li B (2008) Appl Phys Lett 93:163501

[16] Hatch SM, Briscoe J, Dunn S (2013) Adv Mater 25: 867

[17] Tarwal NL, Patil PS (2011) Electrochim Acta 56:6510

[18] Fu M, Li S, Yao J, Wu H, He D, Wang Y (2013) J Porous Mater 20:1485–1489

[19] Xie JS, Wu QS (2010) Mater Lett 64:389-392

[20] Pawinrat P, Mekasuwandumrong O, Panpranot J (2009) Catal Commun 10:1380–1385

[21] Tien LC, Wang HT, Kang BS, Ren F, Sadik PW, Norton DP, Pearton SJ, Lin J (2005) Electro and Solid-State Letters 8 (9): G230-G232

[22] Yogamalar NR, Bose AC, Alloy (2011) J Compd 509:8493

[23] Zhang D, Chava S, Berven C, Lee SK, Devitt R, Katkanant V (2010) Appl Phys A Mater 100:145-150

[24] Zhu G, Yang R, Wang S, Wang ZL (2010) NanoLett 10:3151-3155

[25] Wang T, Jiao Z, Chen T, Li Y, Ren W, Lin Sh, Lu G, Ye J, Bi Y (2013) J Royal Society of Chemistry Nanoscale 5:7552–7557.

[26] Mute A, Peres M, Peiris TC, Lourenço AC, Jensen LR, Monteiro TJ (2010) Nanoscience and Nanotechnology 10:2669-2673

[27] Pauporté T, Bataille G, Joulaud L, Vermersch FJ (2010) J Phys Chem C 114:194-202

[28] Thomas MA, Sun WW and Cui JB (2012) J Phys Chem C 116:6383 −6391

[29] Brayek A, Ghoul M, Souissi A, Ben Assaker I, Lecoq H, Nowak S, Chaguetmi S, Ammar S, Oueslati M, Chtourou R (2014) Materials Letters 129:142–145

[30] Paunovic M, Schlesinger M (2006) Fundamentals of Electrochemical Deposition, John Wiley & Sons, New York

[31] PauporteT, Lupan O, Zhang J, Tugsuz T, Ciofini I, Labat F and Viana B (2015) ACS Appl Mater Interfaces 7:11871 −11880

[32] Lupan O, Cretu V, Postica V, Ahmadi M, Cuenya RB, Chow L, Tiginyanu I, Viana B, Pauporté T, Adelung R (2016) Sensors and Actuators B 223: 893–903

[33] Ghoul M, Braiek B, Brayek A, Ben Assaker I, Khalifa N, Ben Naceur J, Souissi A, Lamouchi A, Ammar S, Chtourou R (2015) J of Alloys and Compounds 647:660-664

[34] Messaoudi O, Makhlouf H, Souissi A, Ben Assaker I, Amiri G, Bardaoui A, Oueslati M, Bechelany M, Chtourou R (2015) Applied Surface Science 343:148–152

[35] Liu J, She J, Deng S, Chen J, Xu N (2008) J Phys Chem C 112:11685

[36] Skompska M, Zarebska K (2014) Electrochim Acta 127:467–488

[37] Wang Y, Li X, Lu G, Quan X, Chen G (2008) J Phys Chem C 112: 7332

[38] Ibănescu M, Muşat V, Textor T, Badilita V, Mahltig B (2014) J Alloy Compd 610:244-249

[39] Joshi MK, Pant HR, Kim HJ, Kim JH, Kim CS (2014) Colloids and Surfaces A, Physicochemical and Engineering Aspects 446:102-108

[40] Hsu MH, Chang CJ (2014) J of Hazardous Materials 278 444–453

[41] Zhu H, Yang D, Zhang H (2006) Mater Letters 60:2686-2689

[42] Cullity BD (1978) Elements of X-ray Diffraction, Second ed. Addison Wesley, Reading, MA 162-165

[43] Pankove JI (1971) Optical Processes in Semiconductors NJ Prentice Hall

[44] Grundmann M (2006) the physics of Semiconductors Springer Com Germany

[45] Sahu DR (2007) J Microelectr 38:1252–1256

[46] Zhou XD, Xiao XH, Xu JX, Cai GX, Ren F, Jiang CZ (2011) EPL (Europhys Lett) 93:57009

[47] Zhu J, Wang Y, Huang L (2005) Mater Chem Phys 93:383–387

[48] Xu J, Zhang ZY, Zhang Y, Lin BX, Fu ZX (2005) Chin Phys Lett 22 :2031

[49] Sun TJ, Qiu JS, Liang CH (2008) J Phys Chem C 112:715–721

[50] Liu HR, Shao GX, Zhao JF, Zhang ZX, Zhang Y, Liang J, Liu XG, Jia HS and Xu BS (2012) J Phys Chem C 116:16182 −16190

[51] Manjón, F.J., Mollar, M., Hernández-Fenollosa, M.A., Marí, B., Lauck, R., Cardona, M. (2003) Solid State Commun 128:35-39

[52] Karyaoui M, Mhamdi A, Kaouach H, Labidi A, Boukhachem A, Boubaker K, Amlouk M, Chtourou R (2015) Mater Sc in Semiconductor Processing 30:255–262

Figure

TABLES

Table 1: EDX data of variation of the anatomical relationship between the zinc and silver for ZnO:Ag Nanowires.

Element	ZnO: 0% Ag	ZnO: 1%Ag	ZnO: 1.5%Ag	ZnO: 2%Ag	ZnO: 3%Ag
Atomic % Zn	100	97.75	96.5	96.15	95.73
Atomic % Ag	0	2.25	3.5	3.85	4.27
Ag+Zn	100	100	100	100	100

Table 2: Crystallite size (D), Crystal parametres (a, c), interplanar spacing (d) for 002 and 101 Miller indexes and microstrain of dislocations (ε) for Ag-ZnO nanowires.

	D (nm)	a (Å)	c (Å)	d (002) (Å)	d (101) (Å)	Strain (ε 10^{-4})
ZnO 0 % Ag	102.22	3.25	5.208	2.604	2.476	20.49
ZnO 1 % Ag	94.88	3.215	5.188	2.579	2.450	21.93
ZnO 1.5 % Ag	85.89	3.228	5.169	2.584	2.459	24.24
ZnO 2 % Ag	78.46	3.223	5.160	2.580	2.455	26.53
ZnO 3 % Ag	71.15	3.221	5.157	2.578	2.453	29.13

a_0= 3.249 Å and c_0= 5.206 Å (JCPDS 036-1451).

FIGURE CAPTIONS

Figure 1. SEM images of ZnO nanowires grown over large surface areas on ITO substrates: a) ZnO nanowires, b, c, d and e) ZnO-Ag nanowires.

Figure 2. Typical EDS spectrum of ZnO NWs: a) undoped ZnO nanowires, b, c, d and e) Ag-decorated ZnO nanowires.

Figure 3a. XRD patterns of ZnO:Ag nanowires (NWs) on an ITO substrate with different Ag doping concentrations (Ag=0,1%,1.5%,2% and 3%).

Figure 3b. Detail of XRD patterns of Ag-decorated ZnO nanowires on ITO substrates with different Ag concentrations (Ag= 0%, 1%, 1.5%, 2% and 3%).

Figure 3c. Crystallite size and residual stress of undoped and Ag-decorated ZnO nanowires prepared by electrodeposition technique.

Figure 4 a-c. Optical transmission (a) and absorption (b) spectra of Ag-decorated ZnO nanowires. Curves correspond to samples (Ag= 0%, 1%, 1.5%, 2% and 3%), respectively. c) Plots of $(\alpha h\nu)^2$ versus energy ($h\nu$) for pure ZnO and ZnO:Ag nanowires.

Figure 5. Photoluminescence spectra of ZnO:Ag nanowires (Ag= 0%, 1%, 1.5%, 2% and 3%).

Figure 6 a-b. Linear sweep voltammograms of the ZnO nanowire (denoted as ZnO NWs) and Ag–ZnO heterostructures (denoted as Ag–ZnO NWs) in the dark (a) and under illumination (b).

Figure 7. Amperometric *I–t* curves of the ZnO nanowire arrays and ZnO:Ag nanowires (Ag= 0%,1%,1.5% and 3%) at an applied voltage of 0.5 V for 20 seconds light on/off cycles.

Figures

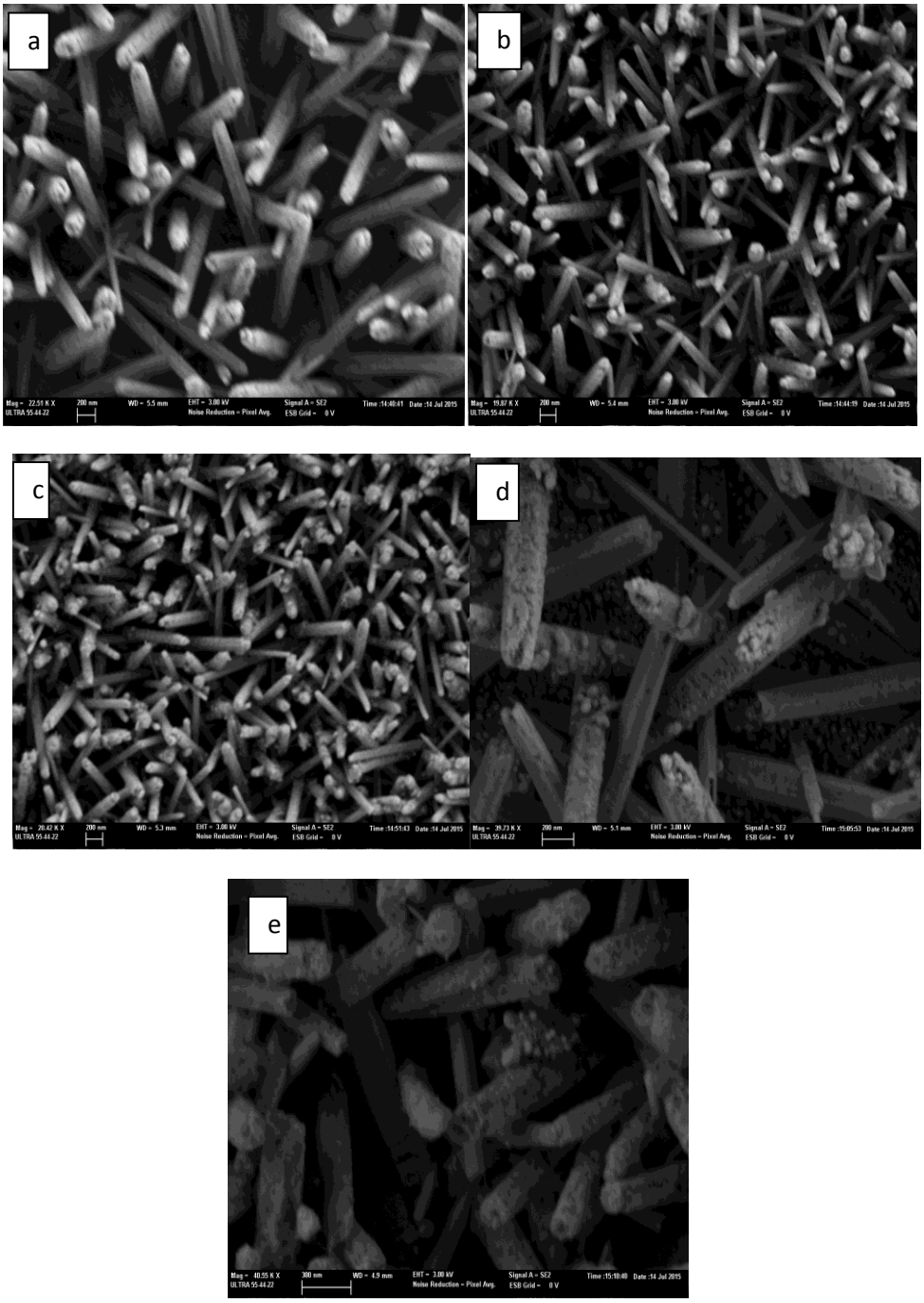

Figure 1. SEM images of ZnO nanowires grown over large surface areas on ITO substrates: a) ZnO nanowires, b, c, d and e) ZnO-Ag nanowires.

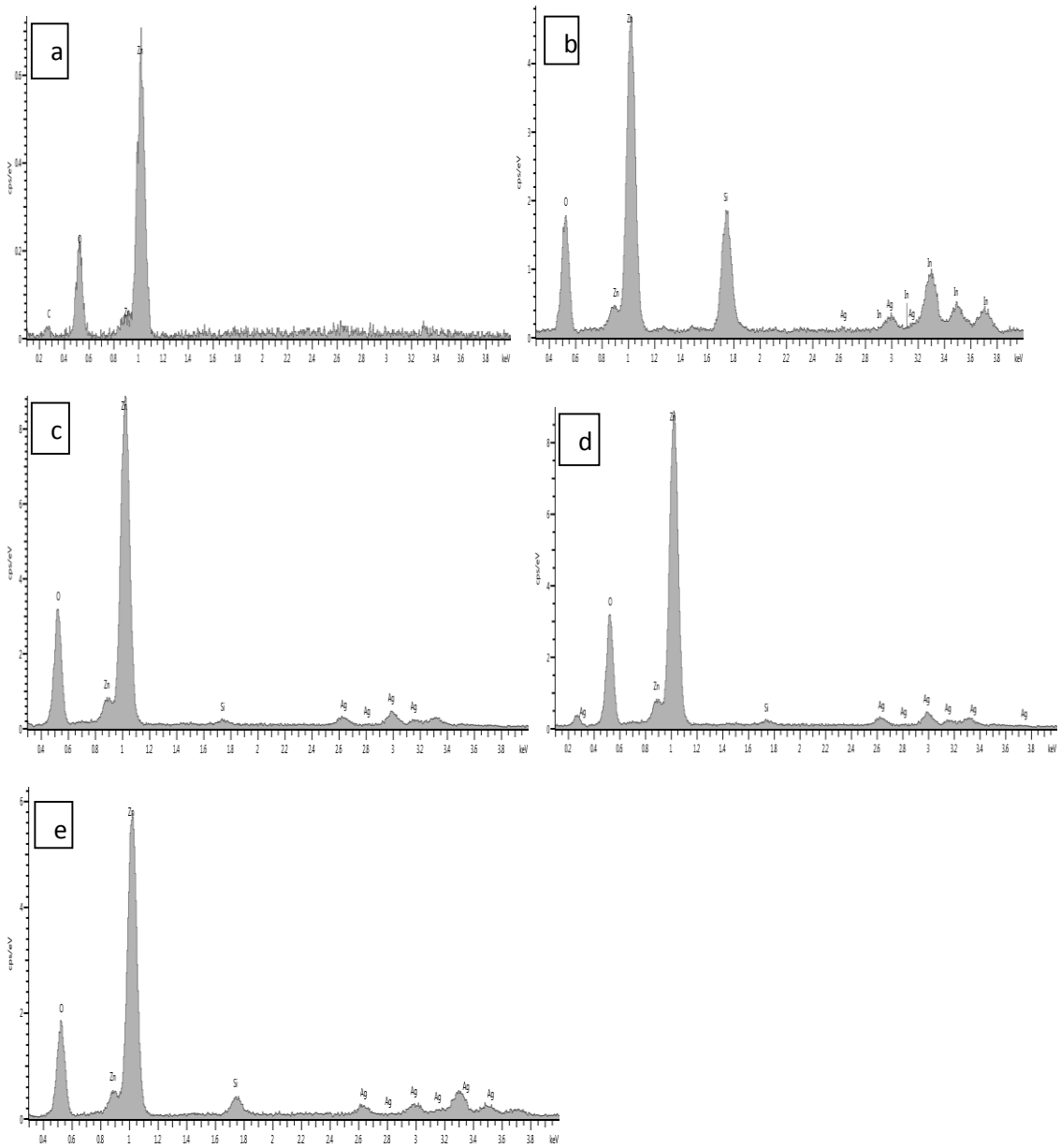

Figure 2. Typical EDS spectrum of ZnO NWs: a) undoped ZnO nanowires, b, c, d and e) Ag-decorated ZnO nanowires.

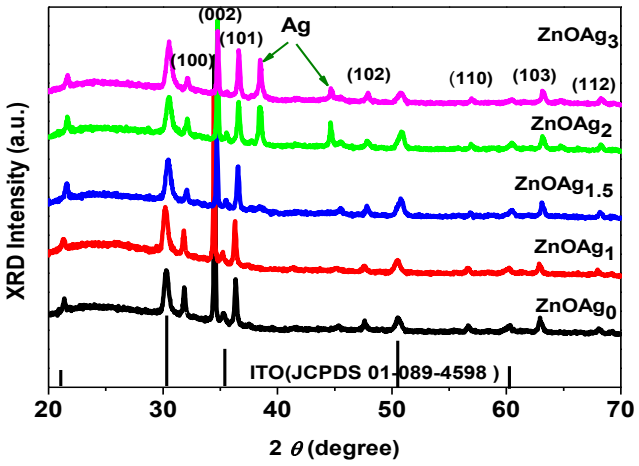

Figure 3a. XRD patterns of ZnO:Ag nanowires (NWs) on an ITO substrate with different Ag doping concentrations (Ag= 0,1,1.5,2 and 3%).

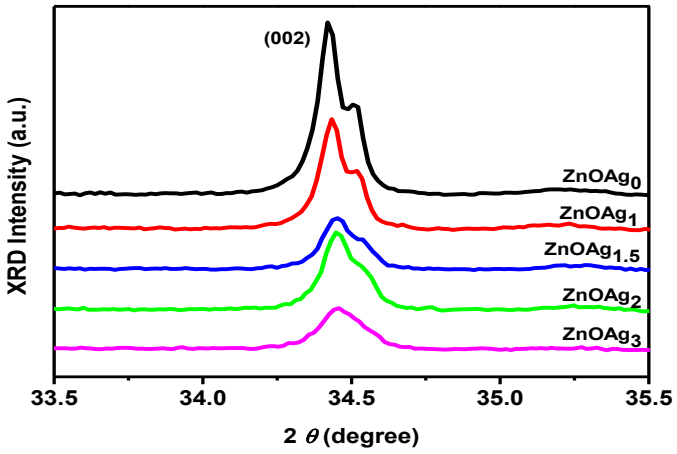

Figure 3b. Detail of XRD patterns of Ag-decorated ZnO nanowires on ITO substrates with different Ag concentrations (Ag= 0, 1, 1.5, 2 and 3%).

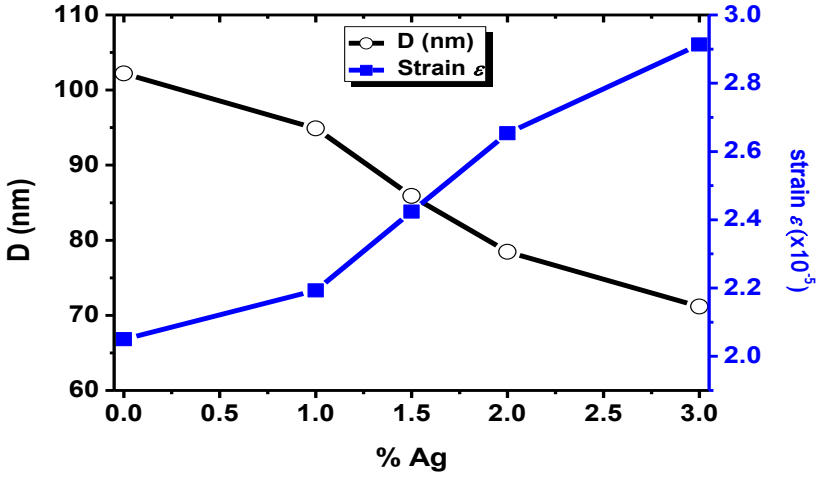

Figure 3c. Crystallite size (D) and residual stress (ε) of undoped and Ag-decorated ZnO nanowires prepared by electrodeposition technique.

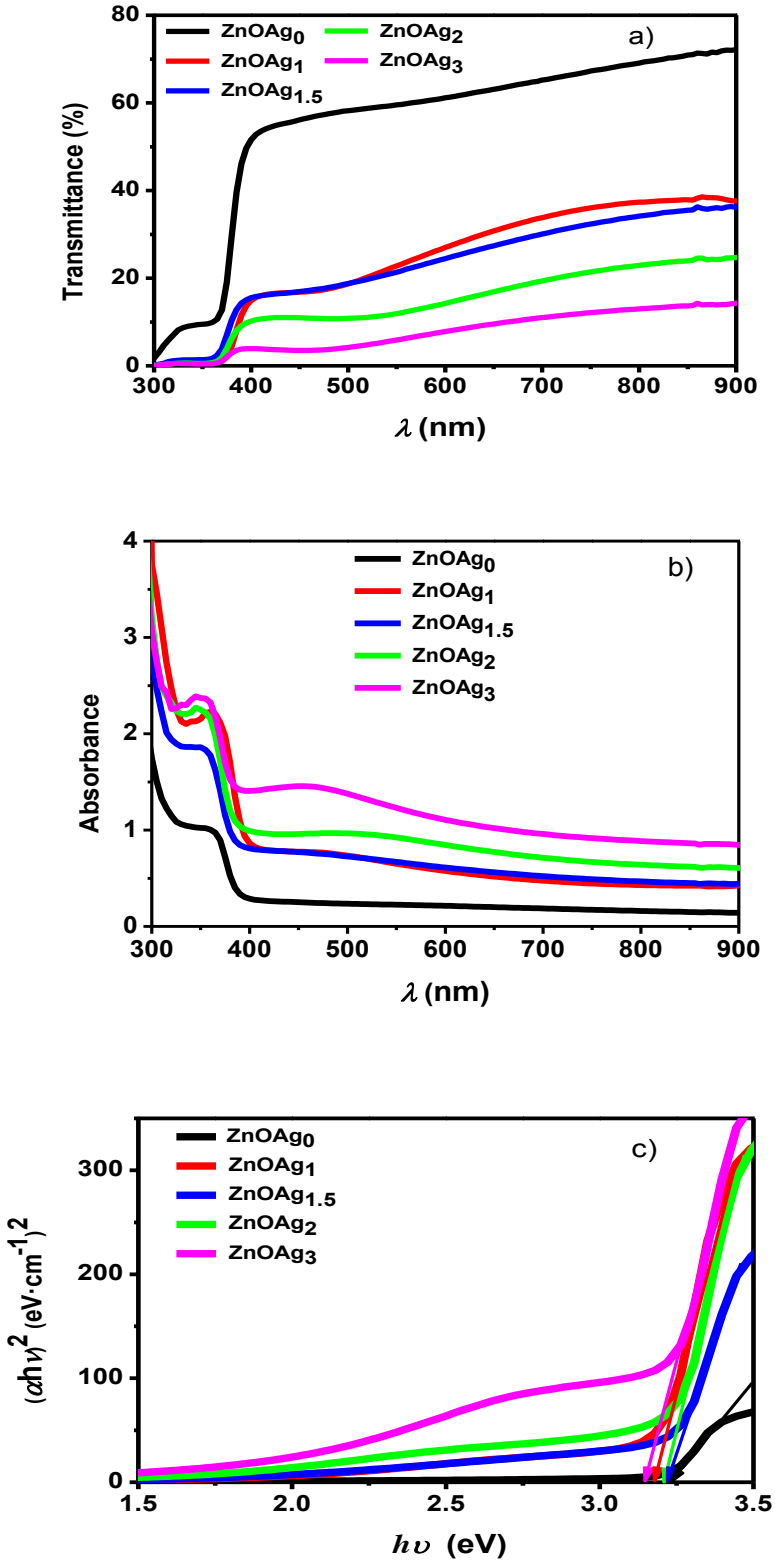

Figure 4 a-c. Optical transmission (a) and absorption (b) spectra of Ag-decorated ZnO nanowires. Curves correspond to samples (Ag= 0, 1, 1.5, 2 and 3%), respectively. c) Plots of $(\alpha h\nu)^2$ versus energy ($h\nu$) for pure ZnO and ZnO:Ag nanowires.

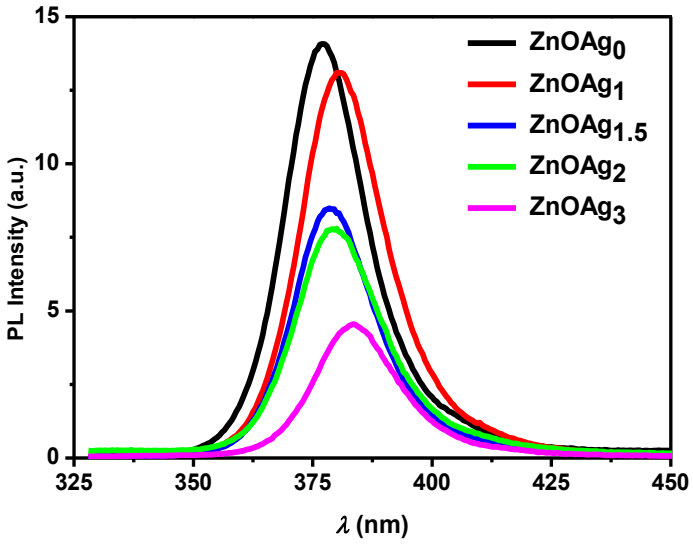

Figure 5. Photoluminescence spectra of ZnO:Ag nanowires (Ag= 0%, 1%, 1.5%, 2% and 3%).

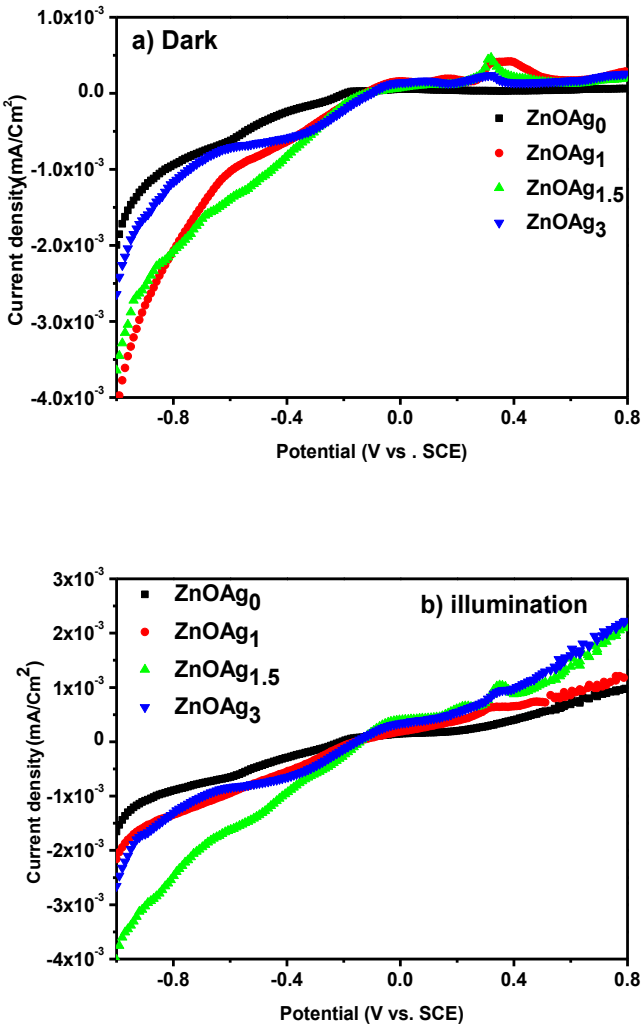

Figure 6 a-b. Linear sweep voltammograms of the ZnO nanowire (denoted as ZnO NWs) and Ag–ZnO heterostructures (denoted as Ag–ZnO NWs) in the dark (a) and under illumination (b).

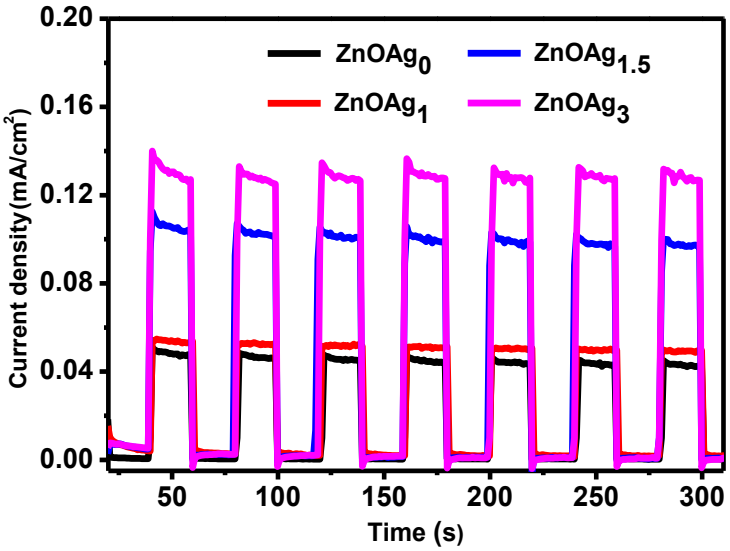

Figure 7. Amperometric *I–t* curves of the ZnO nanowire arrays and ZnO:Ag nanowires (Ag= 0,1,1.5 and 3%) at an applied voltage of 0.5 V for 20 seconds light on/off cycles.